Environ Earth Sci (2012) 65:2161–2178
DOI 10.1007/s12665-011-1196-4

ORIGINAL ARTICLE

GIS-based landslide susceptibility mapping using bivariate statistical analysis in Devrek (Zonguldak-Turkey)

Cagatay Yilmaz · Tamer Topal · Mehmet Lütfi Süzen

Received: 16 April 2010 / Accepted: 2 July 2011 / Published online: 23 July 2011
© Springer-Verlag 2011

Abstract Devrek town with increasing population is located in a hillslope area where some landslides exist. Therefore, landslide susceptibility map of the area is required. The purpose of this study was to generate a landslide susceptibility map using a bivariate statistical index and evaluate and compare the results of the statistical analysis conducted with three different approaches in seed cell concept resulting in different data sets in Geographical Information Systems (GIS) based landslide susceptibility mapping applied to the Devrek region. The data sets are created from the seed cells of (a) crowns and flanks, (b) only crowns, and (c) only flanks of the landslides by using ten different causative parameters of the study area. To increase the data dependency of the analysis, all parameter maps are classified into equal frequency classes based directly on the percentile divisions of each corresponding seed cell data set. The resultant maps of the landslide susceptibility analysis indicate that all data sets produce fairly acceptable results. In each data set analysis, elevation, lithology, slope, aspect, and drainage density parameters are found to be the most contributing factors in landslide occurrences. The results of the three data sets are compared using Seed Cell Area Indexes (SCAI). This comparison shows that the crown data set produces the most accurate and successful landslide susceptibility map of the study area.

Keywords Bivariate analysis · GIS · Landslide susceptibility mapping · Seed cell · Devrek · Turkey

C. Yilmaz · T. Topal (✉) · M. L. Süzen
Department of Geological Engineering, Middle East Technical University, 06531 Ankara, Turkey
e-mail: topal@metu.edu.tr

Introduction

Landslide activity has an increasing trend worldwide, especially in developing countries. Unplanned urbanization and development in unstable hillside areas under the pressures of increasing populations, deforestation, and increased precipitation by changing climates are the main reasons for this increasing trend. Landslide susceptibility maps provide valuable information to planners, developers, and engineers who implement land use strategies not only in the design stages but also in hazard mitigation stages.

There are a number of methods to produce landslide susceptibility maps and several hundreds of paper published in the literature. They are divided into two main categories: qualitative and quantitative approaches (Soeters and Van Westen 1996; Aleotti and Chowdhury 1999; Guzzetti et al. 1999; Ercanoglu et al. 2008; Nandi and Shakoor 2010; Yilmaz 2009a; Bai et al. 2010; Lara and Sepulveda 2010). The qualitative methods extensively used during 1970s and 1980s (Aleotti and Chowdhury 1999) include field geomorphological analysis (Rupke et al. 1988; Concha-Dimas et al. 2007; Kouli et al. 2010) and use of index or parameter maps (Soeters and Van Westen 1996; Van Westen and Lulie 2003), which are generally used by geomorphologists. Quantitative methods include geotechnical engineering approaches, statistical analysis, and soft computing techniques (Aleotti and Chowdhury 1999; Rozos et al. 2008; 2011). The geotechnical approaches use deterministic and probabilistic methods (Gökceoglu and Aksoy 1996; Van Westen and Terlien 1996; Zhou et al. 2003; Wang and Lin 2010). Recently, a number of researchers have used statistical methods, which include bivariate and multivariate analysis. In the bivariate analysis (Fernandez et al. 2003; He et al. 2003; Lin and Tung 2003; Remondo et al. 2003; Cevik and Topal 2003, 2004; Süzen and Doyuran 2004a; Gökceoglu et al. 2005; Saha et al. 2005; Clerici et al. 2002, 2006; Yilmaz and Yildirim 2006; Mathew et al. 2007; Conoscenti et al. 2008; Dahal et al. 2008a, b; Magliulo et al. 2008; Yalcin 2008) each individual factor is combined with landslide distribution map and weight values based on landslide densities are calculated for each parameter class. In the multivariate analysis, many causative factors are sampled and for each of the sampling units, the presence or absence of landslides is also determined. This analysis allows the estimation of the relative weights of each contributing factor by means of statistical procedures (Baeza and Corominas 2001). In the literature, there is a trend to use multivariate statistical analysis such as Discriminant Analysis (Carrara et al. 1991, 2003; Santacana et al. 2003; Guzzetti et al. 2005, 2006a, b; Baeza et al. 2010a), Factor Analysis (Ercanoglu and Gökceoglu 2002; Ercanoglu et al. 2004), Logistic Regression Analysis (Afifi and Clark 1998; Atkinson and Massari 1998; Lee and Min 2001; Dai et al. 2001; Dai and Lee 2002, 2003; Ohlmacher and Davis 2003; Süzen and Doyuran 2004a, b; Ayalew and Yamagishi 2005; Can et al. 2005; Chau and Chan 2005; Yesilnacar and Topal 2005; Wang and Sassa 2005; Lee 2005, 2007a; Duman et al. 2006; Lee and Sambath 2006; Yesilnacar and Süzen 2006; Akgün and Bulut 2007; Chang et al. 2007; Greco et al. 2007; Akgün et al. 2008; Nefeslioglu et al. 2008a, b; Garcia-Rodriguez et al. 2008; Görum et al. 2008; Lamelas et al. 2008; Pradhan et al. 2008; Tunusluoglu et al. 2008; Yao et al. 2008; Chang and Chiang 2009; Mathew et al. 2009; Meusburger and Alewell 2009; Miller et al. 2009; Baeza et al. 2010b; Das et al. 2010; Erener and Düzgün 2010; Oh et al. 2009, 2010; Yilmaz 2010a), and Conditional Analysis (Clerici et al. 2002; Duman et al. 2005; Özdemir 2009). In recent years, researchers frequently use soft computing approaches such as Fuzzy Logic, Artificial Neural Network (ANN), and Neuro-Fuzzy methods (Binaghi et al.1998; Ercanoglu and Gökceoglu 2002, 2004; Lu and Rosembaum 2003; Remondo et al. 2003; Lee et al. 2003a, b, 2004; Tangestani 2004; Ercanoglu 2005; Ermini et al. 2005; Gomez and Kavzoglu 2005; Yesilnacar and Topal 2005; Chang and Chao 2006; Lee et al. 2006; Lee and Evangelista 2006; Kanungo et al. 2006; Lee 2007b; Lee and Pradhan 2007; Chen et al. 2009; Choi et al. 2010; Falaschi et al. 2009; Kanungo et al. 2009; Miles and Keefer 2009; Paliwal and Kumar 2009; Pradhan et al. 2009; Pradhan and Lee 2009, 2010a, b; Yilmaz 2009a, b, 2010b; Akgün and Türk 2010; Pradhan et al. 2010; Rossi et al. 2010).

Black Sea Region, which comprises the northern part of Turkey, has a number of landslides recorded every year. Steep topography and high precipitation make the region very prone to landsliding. Devrek is a town with a population of 22,000 and is located approximately 30 km south of Zonguldak in the western part of the Black Sea Region of Turkey. The settlement area is established in a valley formed by the Devrek Stream. Increasing population causes to spread the urbanization in the hillside areas where some landslides exist. The preparation of landslide susceptibility map of Devrek may serve as useful information to determine the landslide-free areas for future growth and urbanization of the town. The study area is accessible by asphalt paved D750 highway connected to Zonguldak in north and to the Trans European Motorway (TEM) in south (Fig. 1). The study area covers approximately 54 km^2. Devrek region has the climatic characteristics peculiar to the Black Sea region, where summers are chilly, and winters are temperate but cold with rain and snow in higher areas. Precipitation occurs in all four seasons. The annual average precipitation is approximately 170 mm throughout

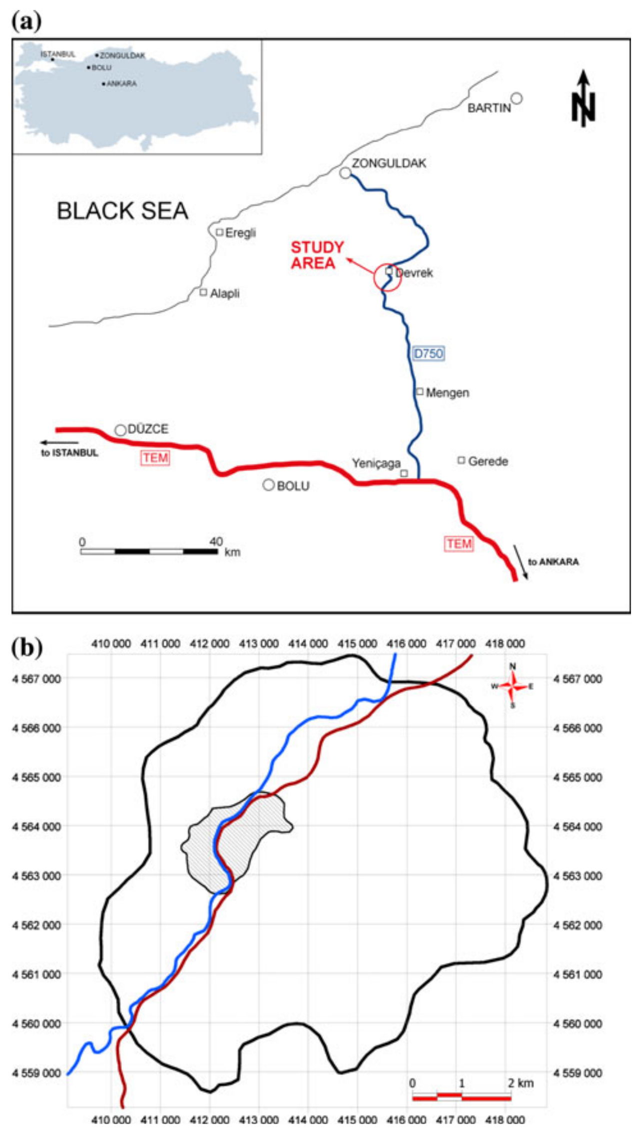

Fig. 1 **a** Location map, and **b** outline of the study area

the region. The average temperature is highest in July with 22.1°C, whereas it is the coldest in January with 4.2°C through the year. The average value of humidity is 71% (DMI 2007). The eastern hillside parts of the study area are partly vegetated with mainly pine and oak trees.

The main goal of this study was to generate a landslide susceptibility map for the Devrek area by using statistical index (Wi) method of Van Westen (1993), which is a bivariate statistical technique utilizing GIS. This method is preferred due to the ease of its application and good performance to predict the susceptible zones. In harmony with this aim, the seed cells are determined and further grouped into three data sets as the data belonging to seed cells of (a) crown and flanks, (b) only crowns, and (c) only flanks. Ten different causative factors are evaluated by three different training sets of seed cells and for each data set a landslide susceptibility map is calculated. The maps are then compared to assess the best one by Seed Cell Area Index method.

Geology and seismicity of the study area

Five lithological units are exposed in the study area (Yergök et al. 1987). From older to younger, they are Kazpınar formation (Early Cretaceous), Alaplı formation (Late Cretaceous), Yahyalar formation (Paleocene), Çaycuma formation (Eocene), and Quaternary alluvial deposits. The geological map and the generalized columnar section of the area are presented in Fig. 2.

The volcanic and volcanoclastic sequence of Kazpınar formation (Krkz) is the oldest geologic unit in the study area. It gives outcrops in the southeastern parts of the study area with pink, partly green to gray andesites with small amounts of tuffs and marls. Andesites dominantly consist of plagioclase crystals with small amounts of hornblendes and biotites.

The Alaplı formation (Kra) overlies the Kazpınar formation by an angular unconformity. The formation consists of an alternating sequence of sandstones, marls, and limestones. The sequence starts with yellow, thick to very thick bedded sandstones. Thin layers of light yellow and red marls overlie the sandstone beds. Above them, there are light yellow to green clayey limestones and limestone beds in moderate thickness. The beds are dipping towards northwest with an average amount of 25°.

The Yahyalar formation (Ty) overlies the Alaplı formation conformably. It consists of an alternating sequence of sandy limestones and sandstones. The sandy limestones are gray to white and thick bedded. The sandstones are gray and thin bedded. The beds dip toward northwest with an average amount of 30°.

The Çaycuma formation (Tç) overlies the Yahyalar formation conformably. It consists of an alternating sequence of sandstones, siltstones, claystones, and volcanoclastic sandstones (Fig. 3). The sandstones are yellow to light green in

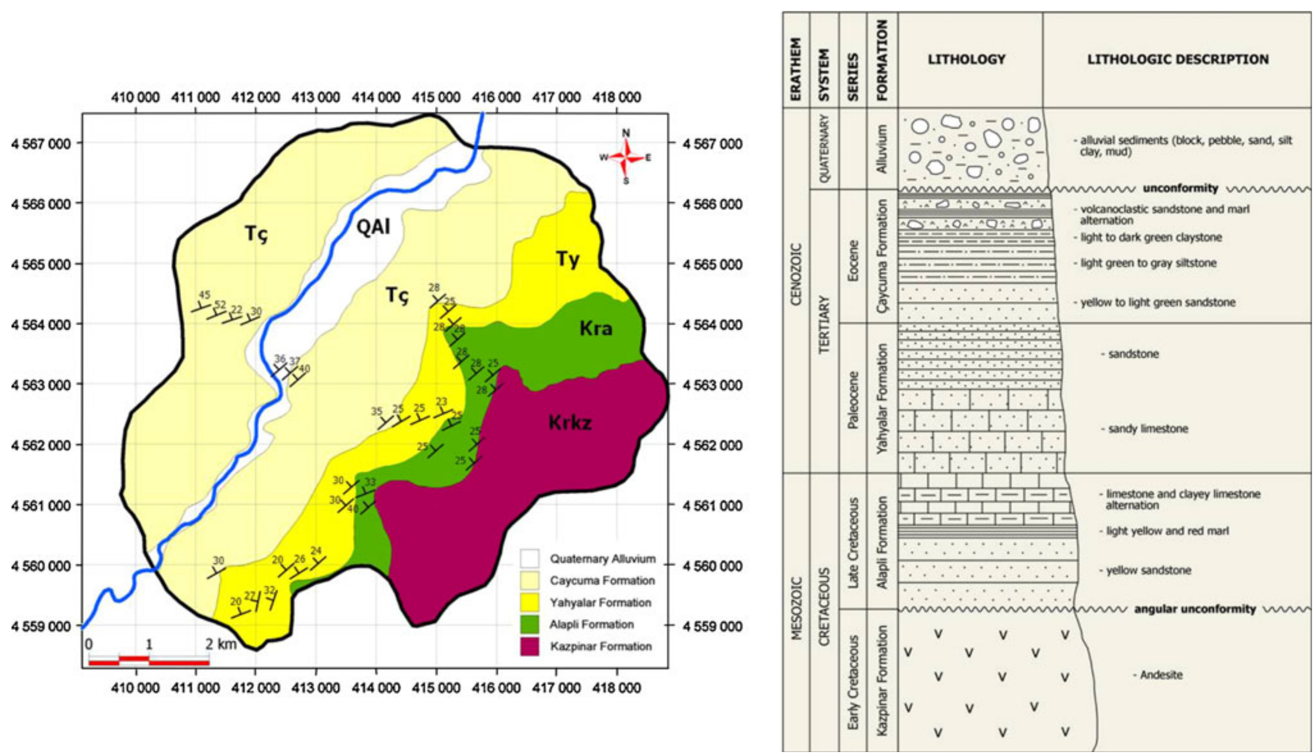

Fig. 2 Geological map and generalized columnar section of the study area (modified from Yergök et al. 1987)

Fig. 3 The alternating sequence in the Çaycuma formation

color and have moderately thick beds. The siltstones are light green to gray and observed as thin layers. The claystones are light to dark green in color and have very thin layers. The volcanoclastic sandstones include agglomerates and tuffs. It is unconsolidated, thin layered, and alternating with thin layers of marls. The beds are dipping towards northwest with an average amount of 35° (Fig. 2).

The Quaternary alluvial deposits (Qal) crop out along the Devrek Stream in the study area. The alluvial fill covers a wide area where the city center of Devrek is located (Fig. 2). The alluvium includes unsorted sediments from mud to block sizes. The coarse components are subangular to round in shape

In the study area, there are no mappable geologic structures such as faults, folds, and lineaments. However, the area lies approximately at 55 km north of the North Anatolian Fault Zone (NAFZ) (Fig. 4a) (MTA 2007). The earthquake activity of this region is directly controlled by the presence and activity of NAFZ, and its associated fault segments. The study area is located within the first-degree earthquake zone of Turkey (GDDA 2007). The distribution of epicenters of past and recent earthquakes are presented in Fig. 4b (KOERI 2007). The study area and its vicinity are seismically not very active, but earthquakes that may occur in the future may trigger landslides. Nevertheless, no information exists about the effect of past earthquakes on landsliding in the study area. Since the study area is relatively small, the effect of seismicity is considered to be equal throughout the area; hence, seismicity is not considered as a parameter in this study.

Methodology and data used

This study was carried out in three main stages; data acquisition, data production and manipulation, analysis and construction of the product (susceptibility) maps. The data acquisition part of the study is based on gathering available geological and topographical maps, and conducting fieldworks to visually inspect the lithologic units and map the landslides in the study area. The geology and geologic map of the study area were gathered mainly from Yergök et al. (1987). During the field investigations, geological map from the literature was checked, the lithologic units were identified, and the landslide inventory map was prepared.

The data production stage consists of data entry, creating the parameter maps, and constructing the databases for the analyses in the next stage. A total of ten parameter maps (elevation, slope, aspect, profile curvature, plan curvature, distance to streams, drainage density, distance to ridges, distance to road and power line network, lithology) were created by utilizing TNT Mips software. The preparation of the data was carried out by using seed cells of Süzen and Doyuran (2004a) for defining the decision rules of slope instabilities, and percentile class divisions for transforming the continuous variables into categorical variables. Seed cells were considered as the best undisturbed morphological conditions before landslide occurs. They were extracted by adding a buffer zone to the crown and flanks of a landslide. In this study, three different sets of seed cell databases were prepared for the analysis as decision rule generators. These seed cells were extracted from the crowns and flanks, only from the crowns, and only from the flanks from the buffer zones added to the landslides in the study area. Then, the continuous data sets extracted from the parameter maps were classified into categories based on percentile divisions of seed cells. The percentile divisions and distributions of seed cells were calculated using SPSS software resulting in reclassification of original parameter maps into percentile maps by using the percentile limits.

For creating the landslide susceptibility maps, statistical index (Wi) method of Van Westen (1993) was used. According to the landslide susceptibility analysis, landslide occurrences in each percentile class for each parameter map were calculated separately. Then, weight values were calculated by comparing the landslide occurrences in each percentile class with the overall landslide occurrence in the parameter map of the study area. The weight values estimate the influence of each causative parameter map. To build the final product maps, the parameter maps were spatially summed up according to their weight values.

Last, the final product maps created using three different seed cell data (from the crowns and flanks, only from the crowns, and only from the flanks) were compared. The results were discussed on the basis of field observations.

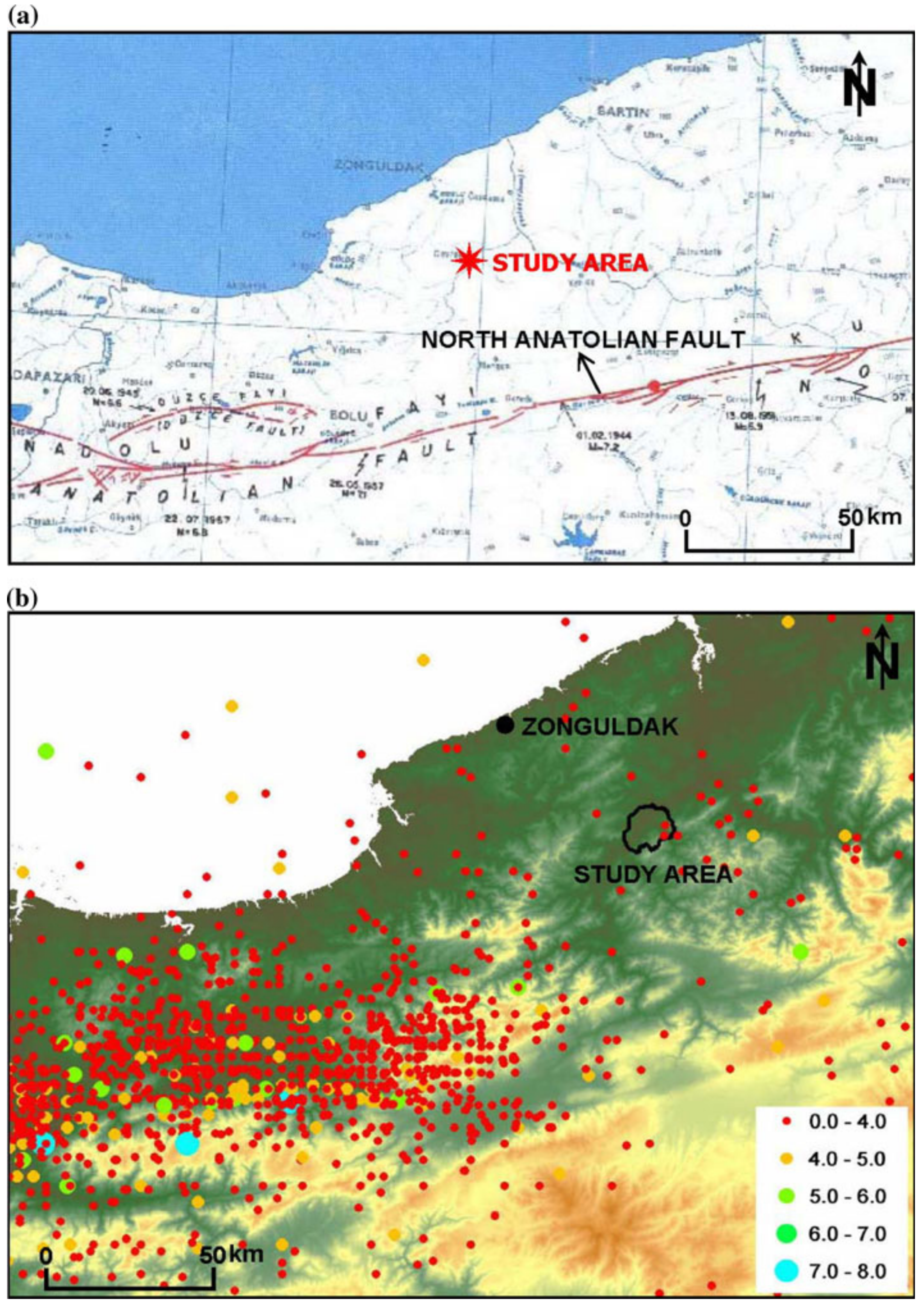

Fig. 4 **a** Map showing the active faults in the western part of Black Sea Region (modified from MTA 2007), and **b** epicenter locations of past and recent earthquakes in the close vicinity of the study area (KOERI 2007)

Production of parameter maps

Landslide inventory map

A landslide inventory map is the simplest output of direct landslide mapping. It shows the location of discernible landslides (Hansen 1984; Wieczorek 1984; Einstein 1988; Van Westen 1994; Parise 2001; Griffiths et al. 2002; Yalcin and Bulut 2007). It is essential for landslide susceptibility mapping since any analysis require a discrete knowledge of which causative factor is effective under what magnitude, which would eventually be derived by overlaying an inventory map with the selected causative factors. A total of 26 active landslides were identified during field work in the study area (Fig. 5). These landslides are classified as slides (Fig. 6). The sliding mechanism of the landslides is rotational, and turns into translational when the sliding mass intersects with the bedding surface of the rock units. The depth of the landslides is generally shallow. They are generally observed at gentle slopes of the Çaycuma formation.

Digital Elevation Model (DEM) and its derivatives

The parameter maps including elevation, slope, aspect, curvature, distance to streams, drainage density and

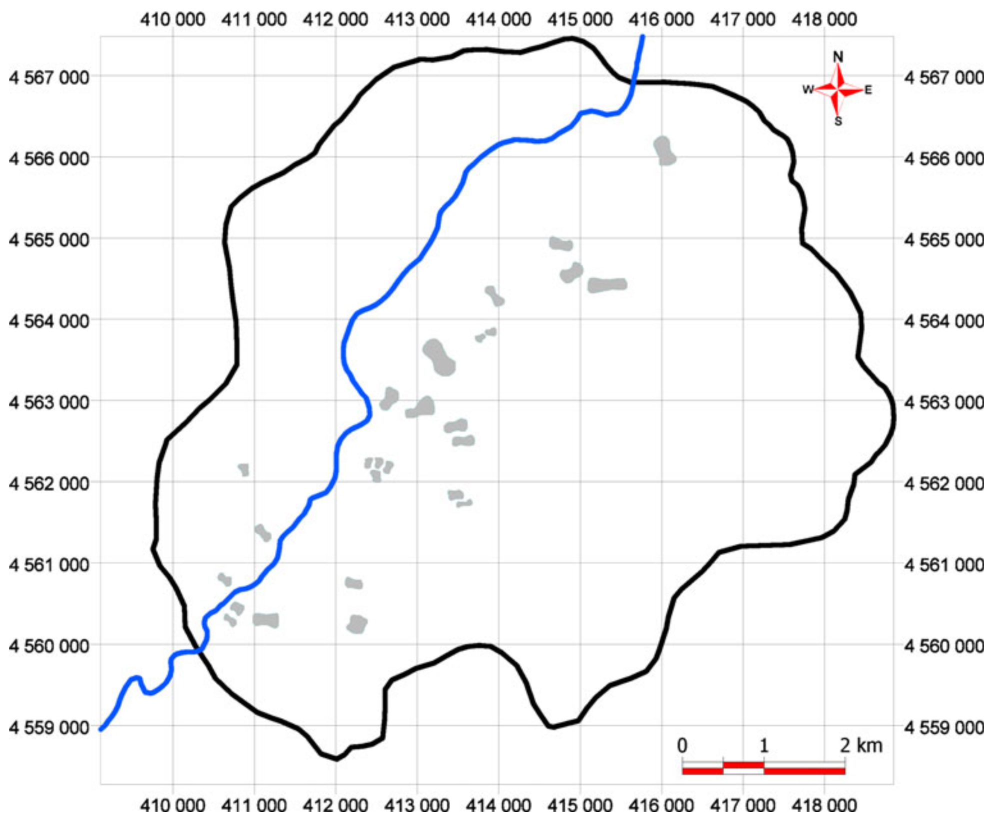

Fig. 5 Landslide inventory map of the study area (grey polygons are landslide bodies)

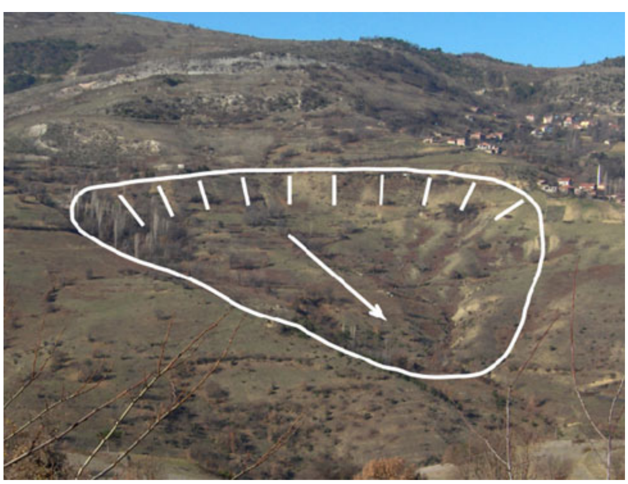

Fig. 6 A landslide occurred near the settlement area. *Arrow* in the figure indicates direction of movement of the landslide

distance to ridges were extracted from the DEM of the study area. The DEM of the study area was constructed from 1:25,000 scale topographical maps with a resolution of 12.5 m.

Elevation map

Elevation is another very frequently used parameter in landslide susceptibility studies (Pachauri and Pant 1992; Ercanoglu et al. 2008). An elevation map portrays areas with different relative relief. Landslides may form in certain relief ranges (Dai et al. 2001). The relief map of the study area with x3 vertical exaggeration generated from the DEM is shown in Fig. 7a.

Slope map

Slope is the measure of surface steepness and measured in degrees. It has a range between 0° and 90°, where 0 represents the flat and 90 represents the vertical areas. Slope angle is very frequently used in landslide susceptibility studies since landsliding is directly related to slope angle (Anbalagan 1992; Pachauri et al. 1998; Saha et al. 2002; Clerici et al. 2002). Landslides mostly occur at certain critical slope angles (Dai et al. 2001; Gökceoglu and Aksoy 1996; Uromeihy and Mahdavifar 2000; Lee and Min 2001; Cevik and Topal 2003). The slope values in the study area (Fig 7b) range between 0^{o} and 63^{o}. However, the mean value of the slope is 17^{o} with a standard deviation of 10^{o}.

Aspect

Aspect is a measure of slope orientation and measured in degrees. Aspect-related parameters such as exposure to sunlight, drying winds, rainfall (degree of saturation), and

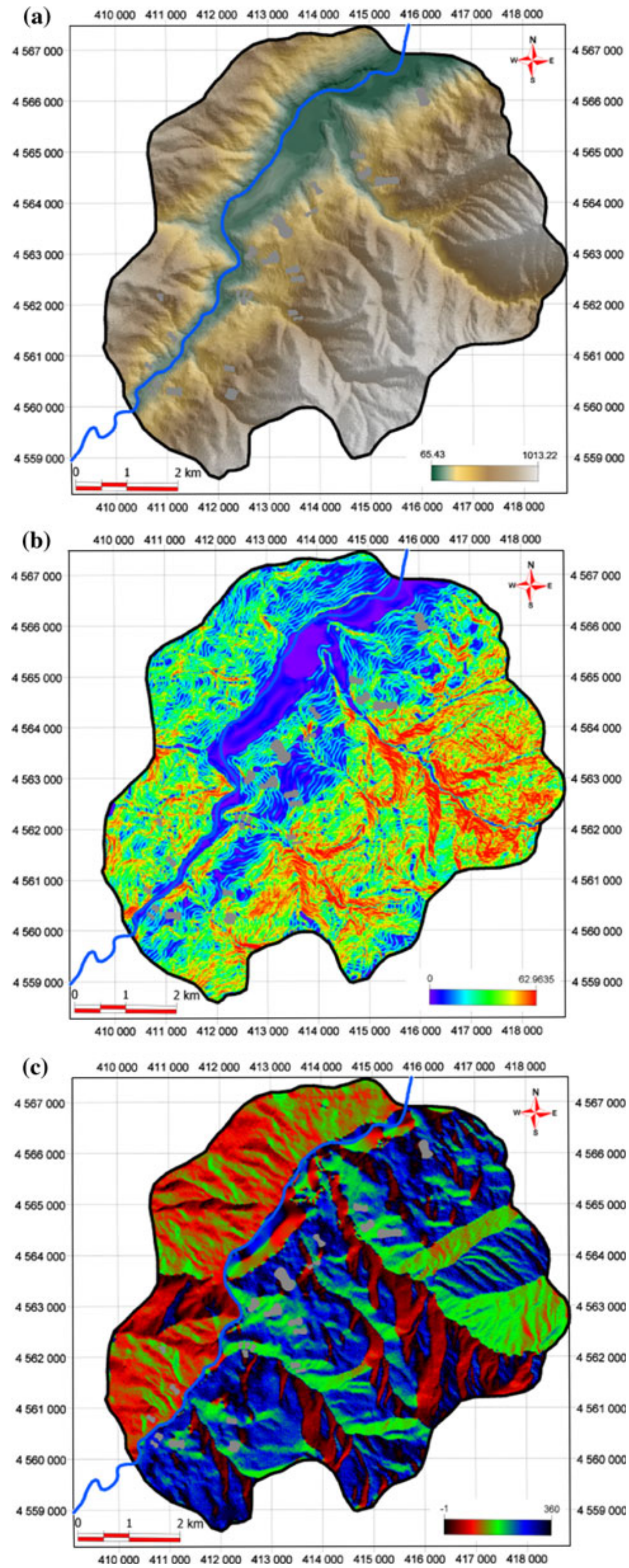

Fig. 7 **a** Relief, **b** slope, and **c** aspect map of the study area

discontinuities may control the occurrence of landslides (Gökceoglu and Aksoy 1996; Dai et al. 2001). The aspect values of the study area vary between −1° and 360° where −1 represents the flat lying areas (Fig. 7c). The mean value of the aspect data is 200 with a standard deviation of 112.

Curvature

Surface curvature is the curvature of a line formed by intersecting a plane (in some chosen orientation) with the terrain surface. The curvature value is the reciprocal of the radius of curvature of the line, so a broad curve has a small curvature and a tight curve has a high curvature value. The curvature is measured in radians per meter.

Profile curvature is the curvature in the vertical plane parallel to the slope direction. It measures the rate of change of slope and therefore influences the flow velocity of water draining the surface and thus erosion and the resulting downslope movement of sediment. Plan curvature (also called contour curvature) is the curvature of a contour line formed by intersecting a horizontal plane with the surface. Plan curvature influences the convergence or divergence of water during downhill flow (MicroImages 2007). Profile curvature raster produced is presented in Fig. 8a. Positive values indicate convex upward surfaces. The values for the study area vary between −0.04 and 0.03. The mean value of the profile curvature data is 0 with a standard deviation of 0.003.

Plan (contour) curvature raster produced for the study is presented in Fig. 8b. Positive values indicate convex outward surfaces. The values vary between −1.8 and 1.5. The mean value of the plan curvature data is 0 with a standard deviation of 0.02.

Derivatives of watershed analysis

The watershed process provides comprehensive processing and evaluation of raster DEMs to define watersheds, flow paths, and basins. The process begins by evaluating the elevation raster for depressions and constructs watershed polygons based on the depressions recognized. The drainage network and ridgelines generated by the watershed analysis are used to produce the parameter maps such as distance to streams, drainage density, and distance to ridges.

The distances of every pixel regarding the streams are calculated and presented in Fig. 9a. The minimum distance of pixels is 0 and the maximum is 545 m. The mean value of the distance to streams data is 107 with a standard deviation of 82.

The streams are also used to calculate the density of streams within every square kilometer in the whole study area. In order to maintain the 1 km^2 search distance, 564 m search radius is used. The vectors of the streams are converted to point data with a distance of 12.5 m and put into point density analysis. The drainage density values of the

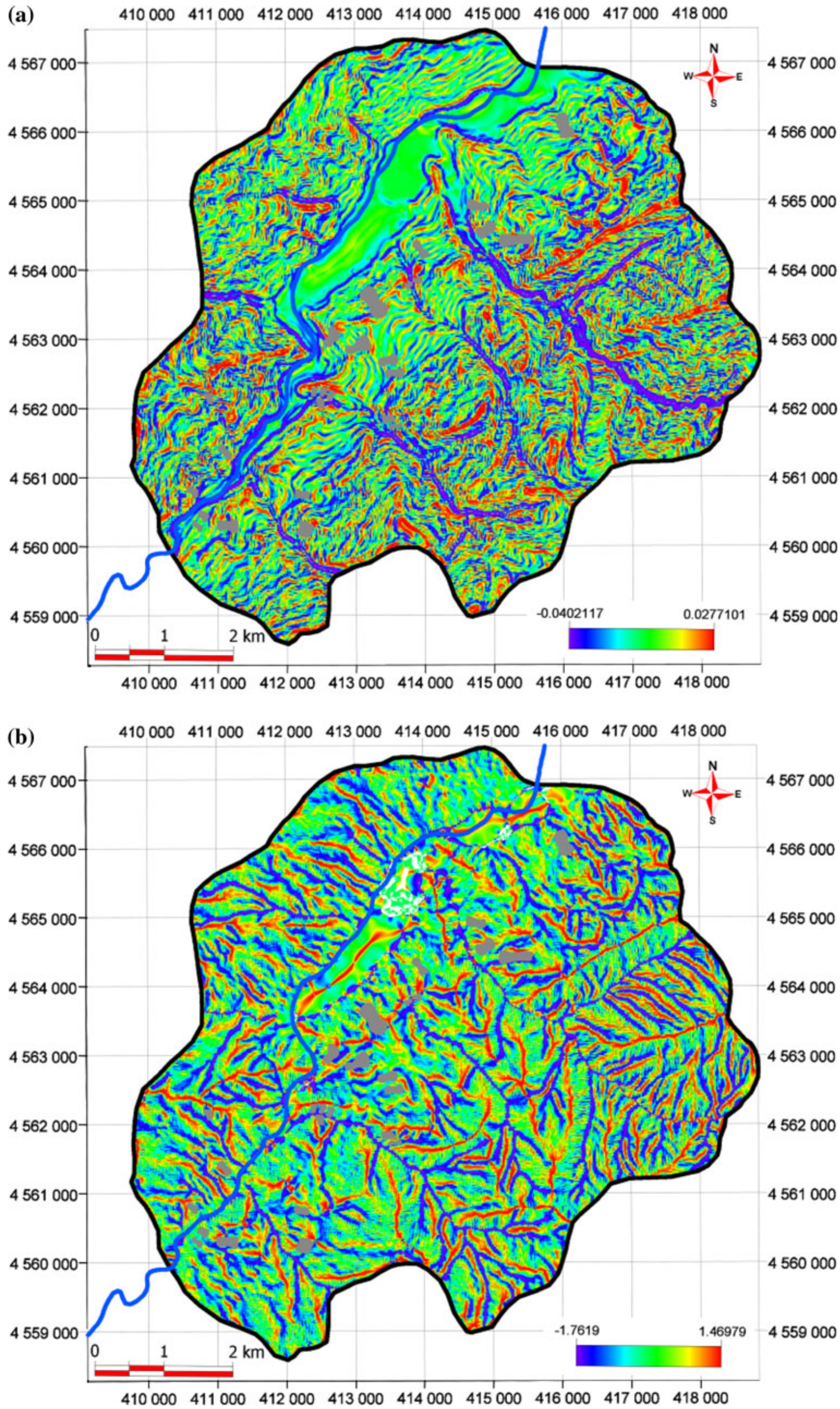

Fig. 8 **a** Profile and **b** plan curvature map of the study area

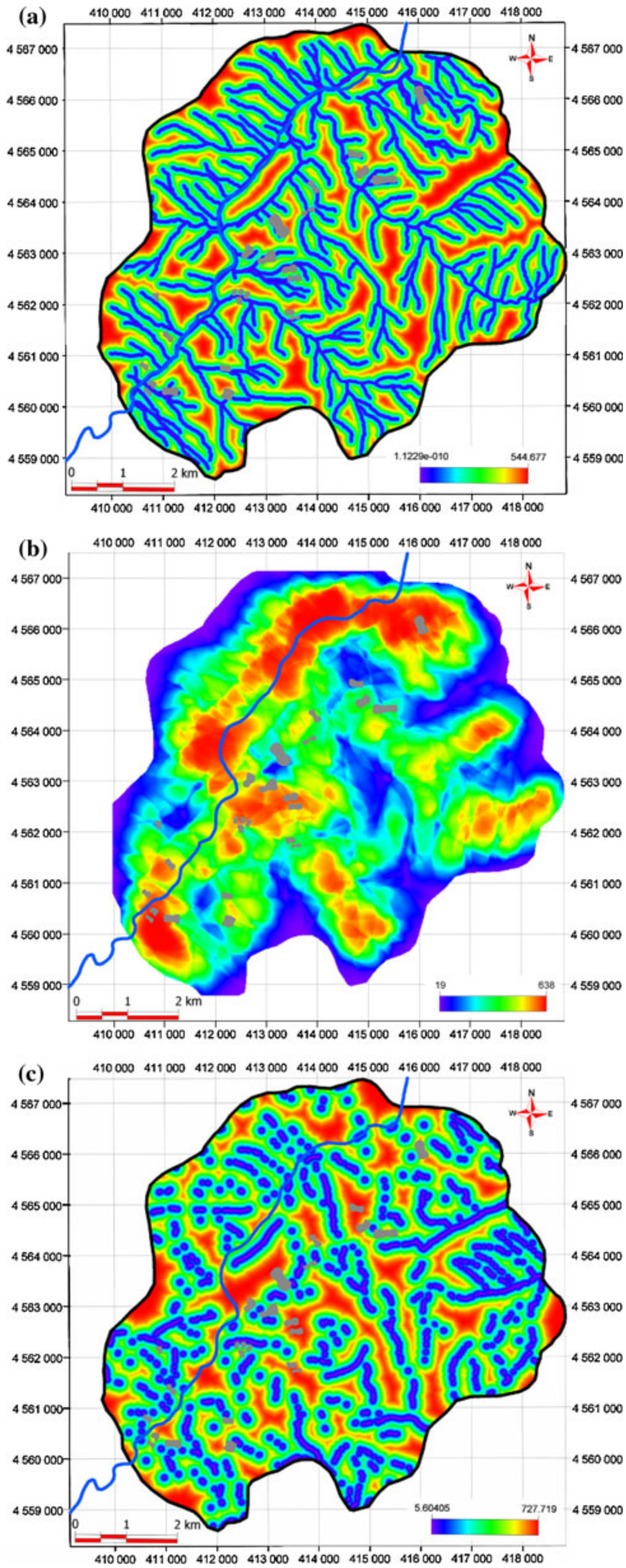

Fig. 9 **a** Distance to streams, **b** drainage density, and **c** distance to ridge map of the study area

study area (Fig. 9b) range from 19 to 638. The mean value of the drainage density data is 293 with a standard deviation of 99.

The ridgelines output of the watershed analysis is used to calculate the nearest distances to the ridges of each pixel. The distance to ridge map is shown in Fig. 9c. The minimum value for the distance to ridges is 6 m and the maximum is 728 m. The distribution has a mean of 168 m with a standard deviation of 110.

Distance to road and power line network

Building the infrastructure elements such as roads (Karslı et al. 2009) and power lines are considered as the man-made activities affecting slope instabilities. For the construction of power line poles, the forest under and in the vicinity of the pylon is cut, so land cover changes, whereas for the road construction both the slopes are cut, the land cover is changed and the economic activity near the roads due to highway tourism attract people that increases the interventions with natural slope.

The roads and power lines in the study area are digitized from the topographical base maps. The vector data of roads and power lines are merged together and the distances of every pixel regarding the roads and power lines are calculated. Distance to road and power line network map of the study area is presented in Fig. 10. The minimum distance of pixels is 0 and the maximum is 746 m. The distribution has a mean of 100 with a standard deviation of 99.

Lithology

The geological map of the study area is compiled from existing geological maps and publications from the literature. The existing maps contain information with some inadequacies and mismatches. So, they were checked and refined during the field study. The compiled map was digitized. Five lithologic units were identified in the study area (Fig. 11). The Çaycuma formation has the greatest areal coverage with almost the half (47.65%) of the study area. Majority of the landslides have occurred in this formation.

Landslide susceptibility analysis

In this study, landslide susceptibility analysis was carried out using the statistical index method (Wi) of Van Westen (1993), which is a bivariate method. For this purpose, landslide inventory, elevation, slope, aspect, profile curvature, plan curvature, distance to streams, drainage density, distance to ridge, distance to road and power line network, and lithology layers were used. Three different

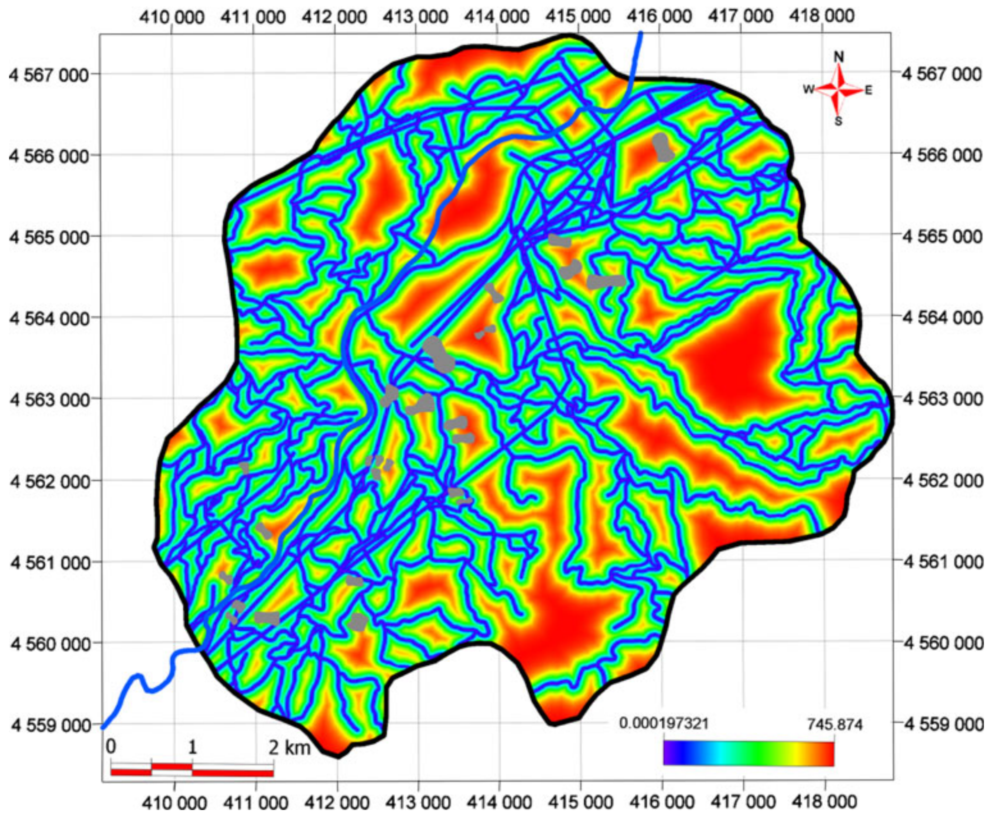

Fig. 10 Distance to road and power line network map of the study area

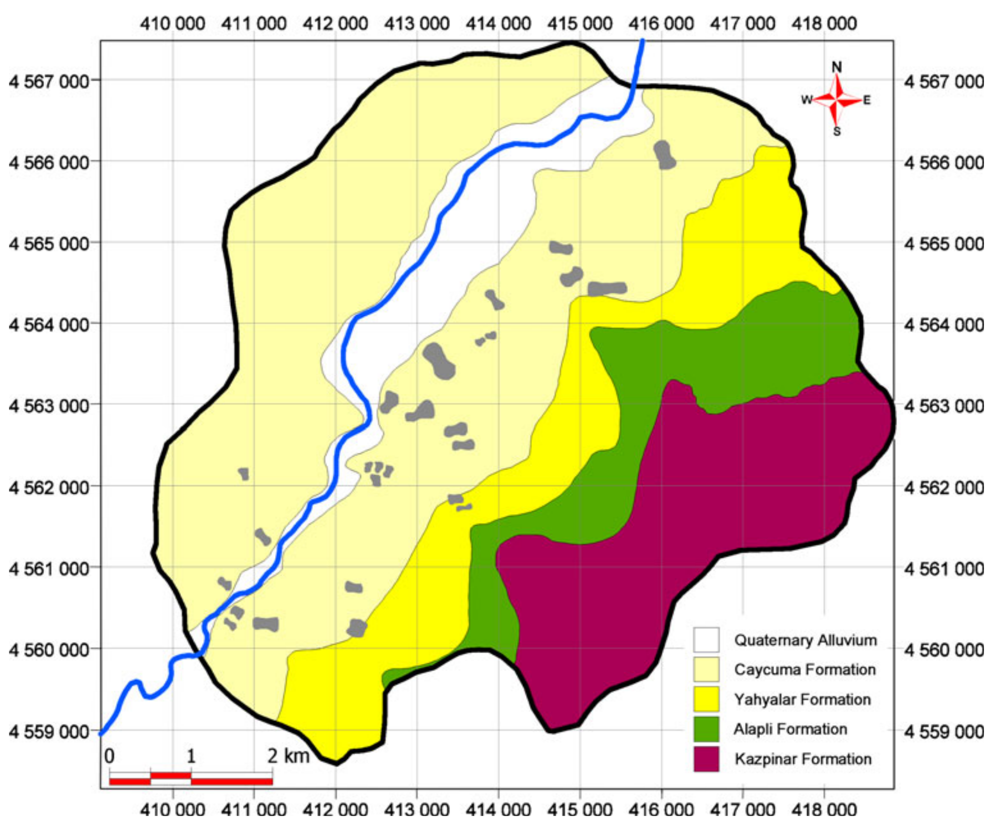

Fig. 11 Geological map showing the lithologic units in the study area presented with landslides (gray polygons) (modified from Yergök et al. 1987)

databases of seed cells were constructed for the bivariate statistical analysis. For the crown and flank database 3,931 seed cell nodes, for the only crowns database 2,289 seed cell nodes, and for the only flanks database 1,642 seed cell nodes were introduced. All seed cell nodes contain data from the ten parameter maps. All parameters except the categorical one (i.e., lithology) were analyzed and reclassified for each seed cell database

In the landslide susceptibility analysis, the occurrence of mass movements is considered as dependent, and parameters are independent variables. Each parameter map (as independent variable) is crossed with landslide distribution map, and weight values, which demonstrate the relative effect of each parameter or variable to instability, are calculated. Weight value for landslide susceptibility is calculated from the landslide density of each class of each parameter map. The landslide density of each class is calculated from following equation:

$$D_{\text{area}} = 1000\frac{Npix(SX_i)}{Npix(X_i)}$$

where D_{area} is the areal density per mileage, $\text{Npix}(\text{SX}_\text{i})$ is the number of pixels with mass movements within variable class X_i, and $\text{Npix}(X_i)$ is the number of pixels within variable class X_i.

The weight value of each control factor class for landslide is defined as the difference between the landslide density of each class and the average landslide density in the study area. The formula for the weight value is

$$W_{\text{area}} = 1000\frac{Npix(SX_i)}{Npix(X_i)} - 1000\frac{\sum Npix(SX_i)}{\sum Npix(X_i)}$$

The calculated weight values are the equal to the degree of susceptibility to landslides of each parameter class. In the presence of a negative weight value, all weights are normalized by adding the absolute value of greatest negative weight to all of the weights of each percentile class. The calculated weights for each percentile class of each parameter for the three different databases, namely crowns and flanks, only crowns, and only flanks, are given in Tables 1, 2, and 3. Based on its categorical nature the

Table 1 Weight values of all parameter classes of the crown and flank database

Parameter class	Parameter								
	Elevation	Slope	Aspect	Profile curv.	Plan curv.	Dist. to streams	Drain. dens.	Dist. to ridges	Dist. to road
10	10.09	5.12	0	0	0	0	0	1.12	0
20	28.41	12.61	1.93	4.78	3.53	1.54	4.99	0	0.79
30	36.83	13.28	18.80	5.87	3.17	5.23	11.10	2.88	1.53
40	29.39	15.71	20.85	4.64	2.87	5.81	16.55	2.98	0.19
50	24.44	15.22	29.69	4.38	1.35	5.95	5.23	2.67	0.11
60	32.72	8.87	20.79	6.43	2.16	4.91	4.71	1.67	3.25
70	19.49	8.69	17.88	5.02	3.39	4.70	13.41	3.55	4.09
80	4.26	6.35	14.46	5.07	4.55	3.79	9.59	3.91	8.56
90	8.53	3.98	6.87	8.14	3.56	4.03	21.20	3.93	9.28
100	0	0	4.66	8.71	7.38	0.51	10.93	26.10	8.12

Table 2 Weight values of all parameter classes of the only crowns database

Parameter class	Parameter								
	Elevation	Slope	Aspect	Profile curv.	Plan curv.	Dist. to streams	Drain. dens.	Dist. to ridges	Dist. to road
10	6.36	3.58	0	0	0	0	0	5.75	0
20	18.25	7.06	1.71	2.31	2.96	0.94	3.24	1.65	1.26
30	14.60	7.39	9.86	3.23	2.05	2.45	6.38	0	1.66
40	13.95	9.23	12.59	2.63	1.56	2.97	12.15	1.10	1.89
50	18.50	9.79	18.86	3.94	0.24	3.03	3.30	2.58	1.24
60	15.87	6.19	13.47	3.30	1.14	3.33	2.24	1.04	0.58
70	4.44	5.09	12.76	3.55	2.89	4.67	6.62	0.97	2.28
80	2.41	2.61	9.01	5.92	2.80	4.66	4.81	2.29	1.58
90	4.96	1.53	3.64	7.51	3.29	5.13	14.92	1.76	1.11
100	0	0	3.03	9.08	5.88	1.30	6.44	12.88	6.24

Table 3 Weight values of all parameter classes of the only flanks database

Parameter class	Parameter								
	Elevation	Slope	Aspect	Profile curv.	Plan curv.	Dist. to streams	Drain. dens.	Dist. to ridges	Dist. to road
10	8.89	2.07	0	0	0.03	0.94	0	0	0.86
20	18.62	4.64	0.42	2.27	0	1.69	1.92	3.76	0.61
30	13.29	5.83	8.45	3.31	0.73	2.69	3.74	3.65	0
40	14.77	5.57	9.32	2.54	1.12	4.52	5.86	2.32	0.31
50	16.77	5.45	11.49	1.81	0.57	4.26	2.36	2.29	1.79
60	12.18	3.56	8.54	1.16	0.59	4.19	2.40	3.10	3.32
70	8.99	3.93	5.91	2.39	1.20	3.12	6.44	4.00	7.66
80	3.83	3.12	29.87	1.89	1.08	1.29	4.73	2.71	10.12
90	5.47	2.22	1.60	0.81	0.15	0.33	7.50	4.53	10.24
100	0	0	1.62	0.38	1.59	0	4.81	14.99	3.39

weights of the Çaycuma formation within lithology layer is calculated separately, where the Çaycuma formation has a weight value of 17.71 for crowns and flanks, of 10.02 for only crowns, and of 7.69 for only flanks.

After calculation of the weights, the weights are assigned to the parameter classes of parameter maps and all ten parameter maps are spatially summed up to create the susceptibility map. The resultant map is then reclassified into four susceptibility classes (very low, low, high, very high) using the susceptibility map distribution parameters. The mean value of the susceptibility map is taken as the pivot point, and classes are assigned to the plus and minus one standard deviations of the distribution.

The distribution of the susceptibility map of crowns and flanks data set results in a mean value of 45.72 and a standard deviation of 21.95. The resultant susceptibility map classified according to these values is presented in Fig. 12a. The ranges and the area covered of the susceptibility classes, and the percentage of seed cells in each susceptibility class for crowns and flanks case are presented in Table 4. According to these results, 44.77% of the study area is classified as high and very high susceptibility, whereas 93.39% of the seed cells are covered within the high and very high susceptibility classes. On the other hand, 55.23% of the study area is classified as low and very low susceptibility with 6.61% of the seed.

The distribution of the susceptibility map of crowns data set results in a mean value of 27.60 and a standard deviation of 12.65. The resultant susceptibility map classified according to these values is presented in Fig. 12b. Table 4 presents the ranges and the area covered of the susceptibility classes, and the percentage of seed cells in each susceptibility class. According to these results, 46.47% of the study area is classified as high and very high susceptibility, while covering 94.71% of the seed cells. On the other hand, 53.53% of the study area is classified as low and very low susceptibility. 5.29% of the seed cells are encountered in these classes.

The distribution of the susceptibility map of flanks data set results in a mean value of 21.21 and a standard deviation of 11.05. The resultant susceptibility map classified according to these values is presented in Fig 12c. Table 4 presents the ranges and the area covered of the susceptibility classes and the percentage of seed cells in each susceptibility class. According to these results, 44.18% of the study area is classified as high and very high susceptibility. 94.15% of the seed cells are in the high and very high susceptibility classes. On the other hand, 55.82% of the study area is classified as low and very low susceptibility. 5.85% of the seed cells are encountered in these classes.

In order to compare the results of the three seed cell databases, Seed Cell Area Index (SCAI) of the susceptibility classes of the maps is calculated (Table 5). SCAI is simply the density of landslides among the classes and is calculated by dividing the susceptibility class area percent values by the landslide seed cell percent values. The logic behind SCAI lies in the correct classification of seed cells within a very conservative areal extent. As a result, it was desired that the high and very high susceptibility classes should have very small SCAI values and low and very low susceptibility classes to have higher SCAI values (Süzen and Doyuran 2004b).

When the SCAI values of the three seed cell data sets are compared, it is seen that the crowns database has the most desirable SCAI values in the very low, low, and very high susceptibility classes. For the high-susceptibility class, the SCAI values are very close to each other, but flanks database has the best result. When the crowns and flanks data sets are compared in terms of the high-susceptibility class, it is found that the crowns database produces a 2.43% greater areal extent than the flanks database with only 1.31% decreases in the landslide seed cells, which could be

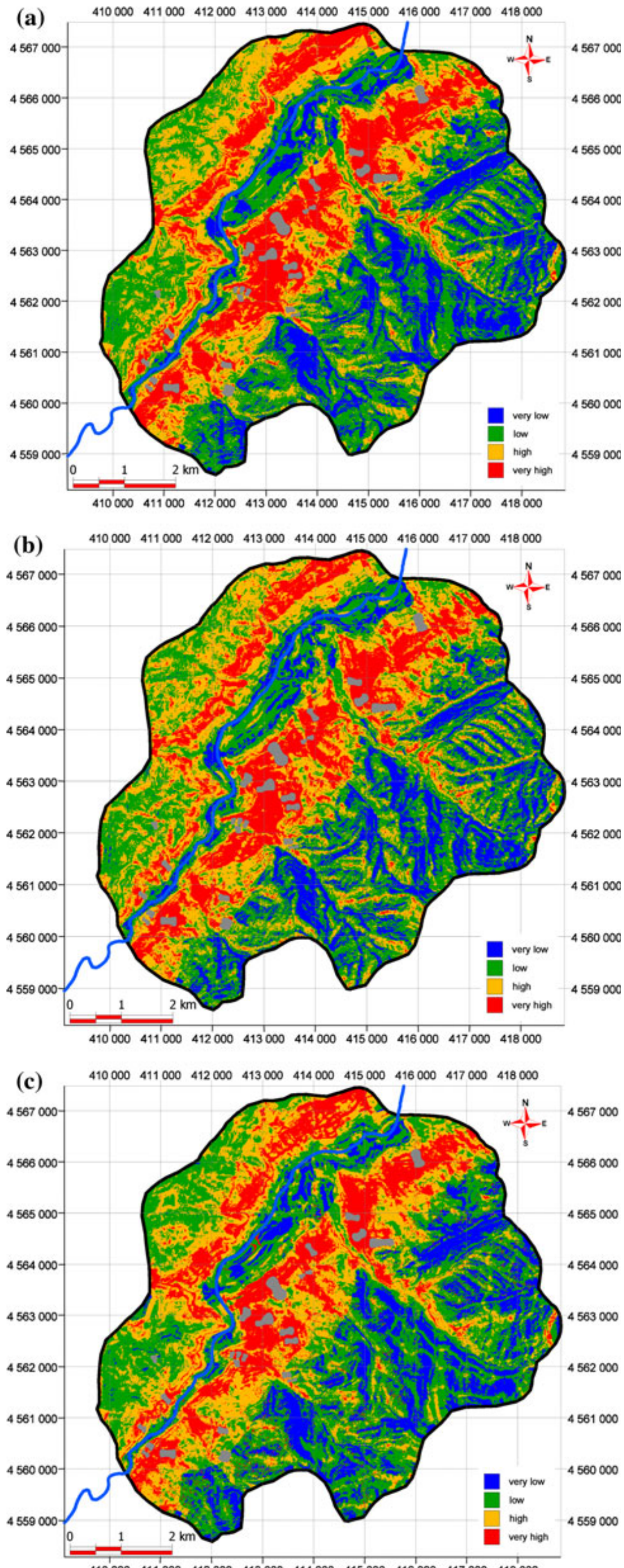

Fig. 12 Landslide susceptibility map of the study area produced from the seed cells of **a** crowns and flanks, **b** only crowns, and **c** only flanks presented with landslides (*grey polygons*)

accepted. As a result of the SCAI analysis, the most accurate and successful map of the study area is produced by the seed cells of crowns.

Discussion

The landslide susceptibility assessment of the Devrek area was carried out using ten different parameters which are generally accepted as landslide contributing factors and widely used in landslide susceptibility assessment studies in the literature. These are lithology, elevation, slope, aspect, profile curvature, plan curvature, distance to streams, drainage density, distance to ridges, and distance to road, and power line network.

The landslide susceptibility assessment was carried out using bivariate statistical method. Besides the scale of the work, statistical method was chosen because of its objectivity and data dependency. However, some procedures in bivariate statistical method are still subjective. Questions arise in the classification of parameter classes and the division of the final susceptibility map into susceptibility classes. To overcome the problem in the classification of parameter classes, percentile method (Süzen and Doyuran 2004a) was applied. Using the percentile method, the parameters were directly classified according to the data itself. On the other hand, the final susceptibility map was divided into susceptibility classes using the susceptibility map distribution. As a result, the objectivity and data dependency of the study were secured.

The analyses of the three data sets resulted in acceptable susceptibility maps since majority of the seed cells falls in high and very high susceptibility classes in each data set. All of the weight values calculated are consistent and reflect no significant extremes which could lead to inconsistencies in the production of susceptibility maps. If the weight values of each parameter class of every attribute are sorted from the highest to the lowest value, elevation, lithology, slope, aspect, and drainage density are found to be the highest contributing factors of landslide occurrence in the study area in all data sets.

The analysis carried out with the crowns and flanks data set indicates that the slopes in the Çaycuma formation with angles from 5° to 17° having altitude values of 139–225 m, and facing to southwest, west and northwest are identified as unstable. Drainage density affects the instability where the drainage density values are from 270 to 300 km^2 and from 357 to 566 km^2. Distance to ridges is the least contributing factor since landslides occurred mostly in the lower parts of hills. In the case of crowns data set, landslide susceptibility accumulates on the slopes of Çaycuma formation with angles from 5° to 16°, which are facing to southwest, west, and northwest at elevations from 150 to

Table 4 The range and areal coverage of the susceptibility classes in the map produced from crowns and flanks, only crown, and only flanks database

Susceptibility class	Crown and flanks			Only crown			Only flanks		
	Range	Area covered (%)	Seed cells (%)	Range	Area covered (%)	Seed cells (%)	Range	Area covered (%)	Seed cells (%)
Very low	0–23.76	17.22	0.10	0–14.94	16.25	0.09	0–10.16	16.58	0.30
Low	23.76–45.72	38.01	6.51	14.94–27.60	37.28	5.20	10.16–21.21	39.24	5.54
High	45.72–67.67	26.78	18.29	27.60–40.25	29.37	19.09	21.21–32.27	26.94	20.40
Very high	67.67–137.40	17.99	75.10	40.25–80.02	17.10	75.62	32.27–89.56	17.24	73.75

Table 5 The densities of landslides among susceptibility classes of the three data sets

Data set	Susceptibility class	Area covered (%)	Seed cell (%)	SCAI
Crowns and flanks	Very low	17.22	0.10	172.20
	Low	38.01	6.51	5.84
	High	26.78	18.29	1.46
	Very high	17.99	75.10	0.24
Crowns	Very low	16.25	0.09	180.56
	Low	37.28	5.20	7.17
	High	29.37	19.09	1.54
	Very high	17.10	75.62	0.23
Flanks	Very low	16.58	0.30	55.27
	Low	39.24	5.54	7.08
	High	26.94	20.40	1.32
	Very high	17.24	73.75	0.23

218 m. Drainage density values range between 268 to 296 and 417 to 566 per square kilometers. Distance to road and power line network parameter has the least effect on the landslide occurrences in the analysis of crowns data set. The results of the flanks data set are also similar to the crowns data set. Instabilities are on the slopes of the Çaycuma formation with angles from 5° to 13° at elevations of 110–210 m, facing to southwest, west and northwest. Drainage density values are from 273 to 307 and from 360 to 537 per square kilometers. Plan curvature parameter has the least effect on the slope instabilities in the case of flanks data set.

All three susceptibility maps are consistent with the field observations. Additionally, in all susceptibility maps, the alluvial deposits of the Devrek Stream are classified as low and very low susceptible. These parts of the area are flat and there is no possibility of landslide occurrence.

Conclusions and recommendations

The field investigation reveal that a total of 26 landslides exist were identified in the Devrek area. They are generally shallow slides, and observed in the Çaycuma formation. The landslide susceptibility analysis using the statistical index method (Wi) of Van Westen (1993) was carried out for seed cells of crowns and flanks, only crowns, and only flanks. The final maps indicate that all data sets produced acceptable results. In all data sets, elevation, lithology, slope, aspect and drainage density were found as the most effective parameters on landslide occurrence of the study area.

Based on the comparison of the susceptibility maps by using the Seed Cell Area Index (SCAI), the map produced from the crowns data set was found as the most accurate and successful landslide susceptibility map of the study area. Seed cells reflect the conditions before landslide occurs and used as decision rules generators for landslide occurrences. Since a landslide starts to be formed at the crown part, choosing only crowns for seed cells might be enough according to the results of this study.

This landslide susceptibility assessment study of the Devrek region may serve as useful information for land use planning. The areas of site-specific studies can be identified and prioritized for detailed geotechnical investigations.

References

Afifi AA, Clark V (1998) Computer aided multivariate analysis. Chapman Hall, London

Akgün A, Bulut F (2007) GIS-based landslide susceptibility for Arsin-Yomra (Trabzon, North Turkey) region. Environ Geol 51:1377–1387

Akgün A, Dag S, Bulut F (2008) Landslide susceptibility mapping for a landslide-prone area (Findikli, NE of Turkey) by likelihood-frequency ratio and weighted linear combination models. Environ Geol 54:1127–1143

Akgün A, Türk N (2010) Landslide susceptibility mapping for Ayvalık (Western Turkey) and its vicinity by multicriteria decision analysis. Environ Earth Sci 61:595–611

Aleotti P, Chowdhury R (1999) Landslide hazard assessment: summary review and new perspectives. Bull Eng Geol Environ 58:21–44

Anbalagan R (1992) Landslide hazard evaluation and zonation mapping in mountainous terrain. Eng Geol 32:269–277

Atkinson PM, Massari R (1998) Generalised linear modelling of susceptibility to landsliding in the Central Appenines, Italy. Comput Geosci 24:373–385

Ayalew L, Yamagishi H (2005) The application of GIS-based logistic regression for landslide susceptibility mapping in the Kakuda–Yahiko Mountains, central Japan. Geomorphology 65:15–31

Baeza C, Corominas J (2001) Assessment of shallow landslide susceptibility by means of multivariate statistical techniques. Earth Surf Proc Land 26:1251–1263

Baeza C, Lantada N, Moya J (2010a) Influence of sample and terrain unit on landslide susceptibility assessment at La Pobla de Lillet, Eastern Pyrenees, Spain. Environ Earth Sci 60:155–167

Baeza C, Lantada N, Moya J (2010b) Validation and evaluation of two multivariate statistical models for predictive shallow landslide susceptibility mapping of the Eastern Pyrenees (Spain). Environ Earth Sci 61:507–523

Bai SB, Wang J, Lü GN, Zhou PG, Hou SS, Xu SN (2010) GIS-based logistic regression for landslide susceptibility mapping of the Zhongxian segment in the Three Gorges area, China. Geomorphology 115:23–31

Binaghi E, Luzi L, Madella P, Pergalani F, Rampini A (1998) Slope instability zonation: a comparison between certainty factor and fuzzy Dempster–Shafer approaches. Nat Hazards 17:77–97

Can T, Nefeslioglu HA, Gökceoglu C, Sönmez H, Duman TY (2005) Susceptibility assessments of shallowearthflows triggered by heavy rainfall at three subcatchments by logistic regression analyses. Geomorphology 72:250–271

Carrara A, Cardinalli M, Detti R, Guzzetti F, Pasqui V, Reichenbach P (1991) GIS techniques and statistical models in evaluating landslide hazard. Earth Surf Proc Land 16:427–445

Carrara A, Crosta GB, Frattini P (2003) Geomorphological and historical data in assessing landslide hazard. Earth Surf Proc Land 28:1125–1142

Cevik E, Topal T (2003) GIS-based landslide susceptibility mapping for a problematic segment of the natural gas pipeline, Hendek (Turkey). Environ Geol 44:949–962

Cevik E, Topal T (2004) Relocation of a problematic segment of a natural gas pipeline using GIS-based landslide susceptibility mapping, Hendek (Turkey), In: Hack R, Azzam R, Charlier R (eds) Proceedings of the 1st European Regional IAEG conference on engineering geology for infrastructure planning in Europe:a European Perspective, pp 265–274

Chang KT, Chiang SH (2009) An integrated model for predicting rainfall-induced landslides. Geomorphology 105:366–373

Chang KT, Chiang SH, Hsu ML (2007) Modeling typhoon- and earthquake-induced landslides in a mountainous watershed using logistic regression. Geomorphology 89:335–347

Chang TC, Chao RJ (2006) Application of back-propagation networks in debris flow prediction. Eng Geol 85:270–280

Chau KT, Chan JE (2005) Regional bias of landslide data in generating susceptibility maps using logistic regression: case of Hong Kong Island. Landslides 2:280–290

Chen CH, Ke CC, Wang CL (2009) A back-propagation network for the assessment of susceptibility to rock slope failure in the eastern portion of the Southern Cross-Island Highway in Taiwan. Env Geol 57:723–733

Choi J, Oh HJ, Won JS, Lee S (2010) Validation of an artificial neural network model for landslide susceptibility mapping. Environ Earth Sci 60:473–483

Clerici A, Perego S, Tellini C, Vescovi P (2002) A procedure for landslide susceptibility zonation by the conditional analysis method. Geomorphology 48:264–349

Clerici A, Perego S, Tellini C, Vescovi P (2006) A GIS-based automated procedure for landslide susceptibility mapping by the Conditional Analysis method: the Baganza valley case study (Italian Northern Apennines). Environ Geol 50:941–961

Concha-Dimas A, Campos-Vargas M, Lopez-Miguel C (2007) Comparing heuristic and bivariate methods for refining landslide susceptibility maps in northern Mexico city. Environ Eng Geosci XIII:277–287

Conoscenti C, Di Maggio C, Rotigliano E (2008) GIS analysis to assess landslide susceptibility in a fluvial basin of NW Sicily (Italy). Geomorphology 94:325–339

Dahal RK, Hasegawa S, Nonomura A, Yamanaka M, Dhakal S, Paudyal P (2008a) Predictive modelling of rainfall-induced landslide hazard in the Lesser Himalaya of Nepal based on weights-of-evidence. Geomorphology 102:496–510

Dahal RK, Hasegawa S, Nonomura A, Yamanaka M, Masuda T, Nishino K (2008b) GIS-based weights-of-evidence modeling in small catchments for landslide susceptibility mapping. Environ Geol 54:311–324

Dai FC, Lee CF (2002) Landslide characteristics and slope instability modeling using GIS, Lantau Island, Hong Kong. Geomorphology 42:213–228

Dai FC, Lee CF (2003) A spatiotemporal probabilistic modelling of storminduced shallow landsliding using aerial photographs and logistic regression. Earth Surf Proc Land 28:527–545

Dai FC, Lee CF, Li J, Xu ZW (2001) Assessment of landslide susceptibility on the natural terrain of Lantau Island, Hong Kong. Env Geol 40:381–391

Das I, Sahoo S, Van Westen C, Stein A, Hack R (2010) Landslide susceptibility assessment using logistic regression and its comparison with a rock mass classification system, along a road section in the northern Himalayas (India). Geomorphology 114:627–637

DMI (2007) Devlet Meteoroloji Isleri Genel Müdürlügü

Duman TY, Can T, Gökceoglu C, Nefeslioglu HA (2005) Landslide susceptibility mapping of Cekmece area (Istanbul, Turkey) by conditional probability. Hydrogeolo Earth Syst Sci Discuss 2:155–208

Duman TY, Can T, Gökceoglu C, Nefeslioglu HA, Sonmez H (2006) Application of logistic regression for landslide susceptibility zoning of Cekmece Area, Istanbul, Turkey. Environ Geol 51:241–256

Einstein HH (1988) Special lecture: landslide risk assessment procedure. In: Bonnrad C (ed) Proceedings of 5th international symposium on landslides, Lausanne. AA Balkema, Rotterdam, pp 1075–1090

Ercanoglu M (2005) Landslide susceptibility assessment of SE Bartin (West Black Sea region, Turkey) by artificial neural networks. Nat Hazards Earth Syst Sci 5:979–992

Ercanoglu M, Gökceoglu C (2002) Assessment of landslide susceptibility for a landslide-prone area (north of Yenice, NW Turkey) by fuzzy approach. Environ Geol 41:720–730

Ercanoglu M, Gökceoglu C (2004) Use of fuzzy relations to produce landslide susceptibility map of a landslide prone area (West Black Sea Region Turkey). Eng Geol 75:229–250

Ercanoglu M, Gökceoglu C, Van Asch ThWJ (2004) Landslide susceptibility zoning of North of Yenice (NW Turkey) by multivariate statistical techniques. Nat Hazards 32:1–23

Ercanoglu M, Kasmer O, Temiz N (2008) Adaptation and comparison of expert opinion to analytical hierarchy process for landslide susceptibility mapping. Bull Eng Geol Environ 67:565–578

Erener A, Düzgün HSB (2010) Improvement of statistical landslide susceptibility mapping by using spatial and global regression methods in the case of More and Romsdal (Norway). Landslides 7:55–68

Ermini L, Catani F, Casagli N (2005) Artificial neural networks applied to landslide susceptibility assessment. Geomorphology 66:327–343

Falaschi F, Giacomelli F, Federici PR, Puccinelli A, D'Amato Avanzi G, Pochini A, Ribolini A (2009) Logistic regression versus artificial neural networks: Landslide susceptibility evaluation in

a sample area of the Serchio River valley, Italy. Nat Hazards 50:551–569
Fernandez T, Irigary C, Hamdouni RE, Chacón J (2003) Methodology for landslide susceptibility mapping by means of a GIS. Application to the Contraviesa Area (Granada, Spain). Nat Hazards 30:297–308
Garcia-Rodriguez MJ, Malpica JA, Benito B, Diaz M (2008) Susceptibility assessment of earthquake-triggered landslides in El Salvador using logistic regression. Geomorphology 95:172–191
GDDA (1997) Earthquake zoning map of Turkey. General Directorate of Disaster Affairs. Ministry of Reconstruction and Resettlement of Turkey, Turkey
Gökceoglu C, Aksoy H (1996) Landslide susceptibility mapping of the slopes in the residual soils of the Mengen Region (Turkey) by deterministic stability analyses and image processing technique. Eng Geol 44:147–161
Gökceoglu C, Sönmez H, Nefeslioglu HA, Duman TY, Can T (2005) The March 17, 2005 Kuzulu landslide (Sivas, Turkey) and landslide susceptibility map of its close vicinity. Eng Geol 81:65–83
Gomez H, Kavzoglu T (2005) Assessment of shallow landslide susceptibility using artificial neural networks in Jabonosa River Basin, Venezuela. Eng Geol 78:11–27
Görum T, Gönencgil B, Gökceoglu C, Nefeslioglu HA (2008) Implementation of reconstructed geomorphologic units in landslide susceptibility mapping: the Melen Gorge (NW Turkey). Nat Hazards 46:323–351
Greco R, Sorriso-Valvo M, Catalano E (2007) Logistic regression analysis in the evaluation of mass movements susceptibility: the Aspromonte case study, Calabria, Italy. Eng Geol 89:47–66
Griffiths JS, Mather AE, Hart AB (2002) Landslide susceptibility in the Rio Aguas catchment, SE Spain. Q J Eng Geol and Hydrogeol 35:9–17
Guzzetti F, Carrara A, Cardinali M, Reichenbach P (1999) Landslide hazard evaluation: a review of current techniques and their application in a multi-scale study, central Italy. Geomorphology 31:181–216
Guzzetti F, Galli M, Reichenbach P, Ardizzone F, Cardinali M (2006a) Landslide hazard assessment in the Collazzone area, Umbria, Central Italy. Nat Hazards Earth Syst Sci 6:115–131
Guzzetti F, Reichenbach P, Ardizzone F, Cardinali M, Galli M (2006b) Estimating the quality of landslide susceptibility models. Geomorphology 81:166–184
Guzzetti F, Reichenbach P, Cardinali M, Galli M, Ardizzone F (2005) Probabilistic landslide hazard assessment at the basin scale. Geomorphology 72:272–299
Hansen A (1984) Landslide hazard analysis. In: Brunsden D, Prior DB (eds) Slope Instability. Wiley, New York, pp 523–602
He YP, Xie H, Cui P, Wei FQ, Zhong DL, Gardner JS (2003) GIS-based hazard mapping and zonation of debris flows in Xiaojiang Basin, Southwestern China. Environ Geol 45:286–293
Kanungo DP, Arora MK, Sarkar S, Gupta RP (2006) A comparative study of conventional, ANN black box, fuzzy and combined neural and fuzzy weighting procedures for landslide susceptibility zonation in Darjeeling Himalayas. Eng Geol 85:347–366
Kanungo DP, Arora MK, Sarkar S, Gupta RP (2009) A fuzzy set based approach for integration of thematic maps for landslide susceptibility zonation. Georisk 3:30–43
Karslı F, Atasoy M, Yalcin A, Reis S, Demir O, Gökceoglu C (2009) Effects of land-use changes on landslides in a landslide-prone area (Ardesen, Rize, NE Turkey). Environ Monit Assess 156:241–255
KOERI (2007) Kandilli seismological data search. Kandilli Observatory and Earthquake Research Institute, Istanbul
Kouli M, Loupasakis C, Soupios P, Vallianatos F (2010) Landslide hazard zonation in high risk areas of Rethymno Prefecture, Crete Island, Greece. Nat Hazards 52:599–621
Lamelas MT, Marinoni O, Hoppe A, Riva J (2008) Doline probability map using logistic regression and GIS technology in the central Ebro Basin (Spain). Env Geol 54:963–977
Lara M, Sepulveda SA (2010) Landslide susceptibility and hazard assessment in San Ramón Ravine, Santiago de Chile, from an engineering geological Approach. Environ Earth Sci 60:1227–1243
Lee S (2005) Application of logistic regression model and its validation for landslide susceptibility mapping using GIS and remote sensing data. Int J Remote Sens 26:1477–1491
Lee S (2007a) Comparison of landslide susceptibility maps generated through multiple logistic regression for three test areas in Korea. Earth Surf Proc Land 32:2133–2148
Lee S (2007b) Application and verification of fuzzy algebraic operators to landslide susceptibility mapping. Env Geol 52:615–623
Lee S, Evangelista DG (2006) Earthquake-induced landslide-susceptibility mapping using an artificial neural network. Nat Hazards Earth Syst Sci 6:687–695
Lee S, Min K (2001) Statistical analysis of landslide susceptibility at Yongin, Korea. Environ Geol 40:1095–1113
Lee S, Pradhan B (2007) Landslide hazard mapping at Selangor, Malaysia using frequency ratio and logistic regression models. Landslides 4:33–41
Lee S, Ryu JH, Lee MJ, Won JS (2003a) Use of an artificial neural network for analysis of the susceptibility to landslides at Boun, Korea. Env Geol 44:820–833
Lee S, Ryu JH, Min K, Won JS (2003b) Landslide susceptibility analysis using GIS and artificial neural network. Earth Surf Proc Land 28:1361–1376
Lee S, Ryu JH, Lee MJ, Won JS (2006) The application of artificial neural networks to landslide susceptibility mapping at Janghung, Korea. Math Geol 38:199–220
Lee S, Ryu JH, Won JS, Park HJ (2004) Determination and application of the weights for landslide susceptibility mapping using an artificial neural network. Eng Geol 71:289–302
Lee S, Sambath T (2006) Landslide susceptibility mapping in the Damrei Romel area, Cambodia using frequency ratio and logistic regression models. Environ Geol 50:847–855
Lin ML, Tung CC (2003) A GIS-based potential analysis of the landslides induced by the Chi–Chi Earthquake. Eng Geol 71:63–77
Lu P, Rosembaum MS (2003) Artificial neural networks and grey systems for the prediction of slope instability. Nat Hazards 30:383–398
Magliulo P, Di Lisio A, Russo F, Zelano A (2008) Geomorphology and landslide susceptibility assessment using GIS and bivariate statistics: a case study in southern Italy. Nat Hazards 47:411–435
Mathew J, Jha VK, Rawat GS (2007) Weights of evidence modelling for landslide hazard zonation mapping in part of Bhagirathi valley, Uttarakhand. Curr Sci 92:628–638
Mathew J, Jha VK, Rawat GS (2009) Landslide susceptibility zonation mapping and its validation in part of Garhwal Lesser Himalaya, India, using binary logistic regression analysis and receiver operating characteristic curve method. Landslides 6:17–26
Meusburger K, Alewell C (2009) On the influence of temporal change on the validity of landslide susceptibility maps. Nat Hazards Earth Syst Sci 9:1495–1507
MicroImages (2007) Terrain curvature. http://www.microimages.com/documentation/cplates/70CurvScript.pdf
Miles SC, Keefer DK (2009) Evaluation of CAMEL-Comprehensive areal model of earthquake-induced landslides. Eng Geol 104:1–15
Miller S, Brewer T, Harris N (2009) Rainfall thresholding and susceptibility assessment of rainfall-induced landslides:

application to landslide management in St Thomas, Jamaica. Bull Eng Geol Environ 68:539–550

MTA (2007) Active fault map of Turkey. http://www.mta.gov.tr/mta_web/dirifay.asp

Nandi A, Shakoor A (2010) A GIS-based landslide susceptibility evaluation using bivariate and multivariate statistical analyses. Eng Geol 110:11–20

Nefeslioglu HA, Duman TY, Durmaz S (2008a) Landslide susceptibility mapping for a part of tectonic Kelkit Valley (Eastern Black Sea Region of Turkey). Geomorphology 94:401–418

Nefeslioglu HA, Gökceoglu C, Sönmez H (2008b) An assessment on the use of logistic regression and artificial neural networks with different sampling strategies for the preparation of landslide susceptibility maps. Eng Geol 97:171–191

Oh H, Lee S, Chotikasathien W, Kim CH, Kwon JH (2009) Predictive landslide susceptibility mapping using spatial information in the Pechabun area of Thailand. Env Geol 57:641–651

Oh HJ, Lee S, Soedradjat GM (2010) Quantitative landslide susceptibility mapping at Pemalang area, Indonesia. Environ Earth Sci 60:1317–1328

Ohlmacher CG, Davis CJ (2003) Using multiple regression and GIS technology to predict landslide hazard in northeast Kansas, USA. Eng Geol 69:331–343

Özdemir A (2009) Landslide susceptibility mapping of vicinity of Yaka Landslide (Gelendost, Turkey) using conditional probability approach in GIS. Env Geol 57:1675–1686

Pachauri AK, Gupta PV, Chander R (1998) Landslide zoning in a part of the Garhwal Himalayas. Env Geol 36:325–334

Pachauri AK, Pant M (1992) Landslide hazard mapping based on geological attributes. Eng Geol 32:81–100

Paliwal M, Kumar UA (2009) Neural networks and statistical techniques: A review of applications. Expert Systems with Applications 36:2–17

Parise M (2001) Landslide mapping techniques and their use in the assessment of the landslide hazard. Phys Chem Earth (C) 26:697–703

Pradhan B, Lee S (2009) Landslide risk analysis using artificial neural network model focusing on different training sites. Int J Phys Sci 3:1–15

Pradhan B, Lee S (2010a) Delineation of landslide hazard areas on Penang Island, Malaysia, by using frequency ratio, logistic regression, and artificial neural network models. Environ Earth Sci 60:1037–1054

Pradhan B, Lee S (2010b) Regional landslide susceptibility analysis using back-propagation neural network model at Cameron Highland, Malaysia. Landslides 7:13–30

Pradhan B, Lee S, Buchroithner MF (2009) Use of geospatial data for the development of fuzzy algebraic operators to landslide hazard mapping: a case study in Malaysia. Applied Geomat 1:3–15

Pradhan B, Lee S, Buchroithner MF (2010) A GIS-based back-propagation neural network model and its cross-application and validation for landslide susceptibility analyses. Comput Environ Urban Syst 34:216–235

Pradhan B, Lee S, Mansor S, Buchroithner MF, Jallaluddin N, Khujaimah Z (2008) Utilization of optical remote sensing data and geographic information system tools for regional landslide hazard analysis by using binomial logistic regression model. J Appl Remote Sens 2:1–11

Remondo J, Gonzalez-Diez A, De Teran JRD, Cendrero A (2003) Landslide susceptibility models utilizing spatial data analysis techniques. A case study from the Lower Deba Valley, Guipuzcoa (Spain). Nat Hazards 30:267–279

Rossi M, Guzzetti F, Reichenbach P, Mondini A, Peruccacci S (2010) Optimal landslide susceptibility zonation based on multiple forecasts. Geomorphology 114:129–142

Rozos D, Pyrgiotis L, Skias S, Tsagaratos P (2008) An implementation of rock engineering system for ranking the instability potential of natural slopes in Greek territory. An application in Karditsa County. Landslides 5:261–270

Rozos D, Bathrellos GD, Skillodimou HD (2011) Comparison of the implementation of rock engineering system (RES) and analytic hierarchy process (AHP) methods, upon landslide susceptibility mapping, using GIS: a case study from the Eastern Achaia County of Peloponnesus, Greece. Environ Earth Sci. doi: 10.1007/s12665-010-0687-z

Rupke J, Cammeraat E, Seijmonsbergen AC, Van Westen CJ (1988) Engineering geomorphology of Widentobel Catchment, Appenzell and Sankt Gallen, Switzerland: a geomorphological inventory system applied to geotechnical appraisal of slope stability. Eng Geol 26:33–68

Saha AK, Gupta RP, Arora MK (2002) GIS-based landslide hazard zonation in the Bhagirathi (Ganga) valley, Himalayas. Int J Remote Sens 23:357–369

Saha AK, Gupta RP, Sarkar I, Arora MK, Csaplovics E (2005) An approach for GIS-based statistical landslide susceptibility zonation—with a case study in the Himalayas. Landslides 2:61–69

Santacana N, Baeza B, Corominas J, Paz AD, Marturia (2003) A GIS-based multivariate statistical analysis for shallow landslide susceptibility mapping in la Pobla de Lillet Area (Eastern Pyrenees, Spain). Nat Hazards 30:281–295

Soeters R, Van Westen CJ (1996) Slope instability recognition analysis and zonation. In: Turner KT, Schuster RL (eds) Landslides: investigation and mitigation. Transportation Research Board National Research Council, Special Report, Washington, DC, pp 129–177

SPSS (2003) Statistical package for the Social Sciences

Süzen ML, Doyuran V (2004a) Data driven bivariate landslide susceptibility assessment using geographical information systems: a method and application to Asarsuyu catchment, Turkey. Eng Geol 71:303–321

Süzen ML, Doyuran V (2004b) A comparison of the GIS based landslide susceptibility assessment methods Multivariate versus bivariate. Environ Geol 45:665–679

Tangestani MH (2004) Landslide susceptibility mapping using the fuzzy gamma approach in a GIS, Kakan catchment area, southwest Iran. Aust J Earth Sci 51:439–450

TNT Mips (2004) TNT Mips Manual: processes

Tunusluoglu MC, Gökceoglu C, Nefeslioglu HA, Sönmez H (2008) Extraction of potential debris source areas by logistic regression technique: a case study from Barla, Besparmak and Kapi mountains (NW Taurids, Turkey). Env Geol 54:9–22

Uromeihy A, Mahdavifar MR (2000) Landslide hazard zonation of the Khorshrostam area, Iran. Bull Eng Geol Environ 58:207–213

Van Westen CJ (1993) Application of geographic information systems to landslide hazard zonation. ITC Publication No: 15. International Institute for Aerospace and Earth Resources Survey, Enschede

Van Westen CJ (1994) GIS in landslide hazard zonation: a review, with examples from the Andes of Colombia. In: Price MF, Heywood DI (eds) Geographical information systems in landslide hazard zonation GIS applications for mountain areas. Taylor and Francis, London, pp 135–165

Van Westen CJ, Lulie GF (2003) Analyzing the evolution of the Tessina landslide using aerial photographs and digital elevation models. Geomorphology 54:77–89

Van Westen CJ, Terlien TJ (1996) An approach towards deterministic landslide hazard analysis in GIS. A case study from Manizales (Colombia). Earth Surf Proc Land 21:853–868

Wang HB, Sassa K (2005) Comparative evaluation of landslide susceptibility in Minamata area, Japan. Environ Geol 47:956–966

Wang KL, Lin ML (2010) Development of shallow seismic landslide potential map based on Newmark's displacement: the case study of Chi–Chi earthquake, Taiwan. Environ Earth Sci 60:775–785

Wieczorek GF (1984) Preparing a detailed landslide-inventory map for hazard evaluation and reduction. Bull Assoc Eng Geol 21:337–342

Yalcin A (2008) GIS-based landslide susceptibility mapping using analytical hierarchy process and bivariate statistics in Ardesen (Turkey): comparisons of results and confirmations. Catena 1:1–12

Yalcin A, Bulut F (2007) Landslide susceptibility mapping using GIS and digital photogrammetric techniques: a case study from Ardesen (NE-Turkey). Nat Hazards 41:201–226

Yao X, Than LG, Dai FC (2008) Landslide susceptibility mapping based on Support Vector Machine: a case study on natural slopes of Hong Kong. Geomorphology 101:572–582

Yergök AF, Akman Ü, İplikci E, Karabalik N, Keskin İ, Mengi H, Umut M, Armagan F, Erdogan K, Kaymakci H, Cetinkaya A (1987) Batı Karadeniz bölgesinin jeolojisi, MTA Rapor No: 8273 (unpublished)

Yesilnacar E, Süzen ML (2006) A land-cover classification for landslide susceptibilty mapping by using feature components. Int J Remote Sens 27:253–275

Yesilnacar E, Topal T (2005) Landslide susceptibility mapping: A comparison of logistic regression and neural Networks methods in a medium scale study, Hendek region (Turkey). Eng Geol 79:251–266

Yilmaz I (2009a) A case study from Koyulhisar (Sivas-Turkey) for landslide susceptibility mapping by artificial neural networks. Bull Eng Geol Environ 68:297–306

Yilmaz I (2009b) Landslide susceptibility using frequency ratio, logistic regression, artificial neural networks and their comparison: a case study from Kat landslides (Tokat-Turkey). Comput Geosci 35:1125–1138

Yilmaz I (2010a) Comparison of landslide susceptibility mapping methodologies for Koyulhisar, Turkey: conditional probability, logistic regression, artificial neural networks, and support vector machine. Environ Earth Sci 61:821–836

Yilmaz I (2010b) The effect of the sampling strategies on the landslide susceptibility mapping by conditional probability (CP) and artificial neural networks (ANN). Environ Earth Sci 60:505–519

Yilmaz I, Yildirim M (2006) Structural and geomorphological aspects of the Kat landslides (Tokat-Turkey), and susceptibility mapping by means of GIS. Env Geol 50:461–472

Zhou G, Esaki T, Mitani Y, Xie M, Mori J (2003) Spatial probabilistic modeling of slope failure using an integrated GIS Monte Carlo simulation approach. Eng Geol 68:373–386